



Full Length Article

Relationship between fly ash nanoparticle-stabilized-foam and oil production in core displacement and simulation studies

Guan Ming Phong^a, Rashidah M. Pilus^{a,*}, Afiq Mustaffa^a, Lakshmi Priya Thangavel^b, Norani Muti Mohamed^b

^a Department of Petroleum Engineering, Universiti Teknologi Petronas, Malaysia

^b Department of Applied Science, Universiti Teknologi Petronas, Malaysia



ARTICLE INFO

Keywords:

Nanoparticles
Fly ash
FAWAG
Foam
EOR

ABSTRACT

In this study, the use of coal fly ash nanoparticles as a stabilizer to generate stable foam was explored. First, the fly ash nanoparticles will undergo two-step chemical treatment to synthesize a smaller nanoparticle of higher purity. The fabricated nanoparticle's size was 50 nm and the composition was 99% zeolites and 1% sodium compounds were characterized using Field-Emission Scanning Electron Microscope (FESEM), Energy-Dispersive X-ray Spectroscopy (EDX) and X-ray Photoelectron Spectrometer (XPS). Static foam stability test was done to screen the type and concentration of nanoparticle that has the potential for a foam stabilizer for further core displacement tests. The highest half-life of foam was by fabricated nanoparticles (FN) with a concentration of 80:20 at 875 s. The core displacement test was done to determine the effectiveness of fly ash nanoparticles on oil recovery. The oil recovery results showed that foam with the presence of FN nanoparticles produced a higher oil recovery than those without nanoparticles. The mobility reduction factor (MRF) value of foam with nanoparticles was two times higher than foam without nanoparticles. A sensitivity analysis is done to determine whether the factor governing oil recovery and MRF is the foam stability or surfactant adsorption. The oil recovered by foam injection increased by 30.69% when the surfactant adsorption was reduced by 75%, however, the oil recovery was only half of this value when the foam half-life was tripled. This may indicate that surfactant adsorption is still a major influence to be monitored on increasing oil recovery while focusing on foam stability.

1. Introduction

Gas Injection is one of the widely applied EOR injection methods other than water injection [1–4] because the sweep efficiency of water injection across the porous media is much lower than gas injection [5]. However, due to the inefficiency of gas injection in reservoir conditions, this method is not often promising due to the low density and viscosity characteristics of gas compared to water and crude oil [6]. These characteristics lead to gas injection suffering from the effect of viscous fingering and gravity segregation leading to early gas breakthrough and low oil recovery. Additionally, reservoir heterogeneity further contributes to poor volumetric sweep efficiency [7]. To alleviate the drawbacks of gas injection, foam injection is proposed to improve the oil recovery as it can reduce the viscous fingering and gravity segregation. The objective of foam application is to increase the displacing fluid viscosity and density for the fluid to achieve a more favorable mobility ratio during gas flooding. In other words, the foam serves as a mobility control agent in gas flooding [8,9]. Foam helps to reduce the

high mobility of gas phase in the porous media [10,11]. This is because in the form of foam, the gases are trapped in the foam and thus, the more stable foam further reduces the gas mobility in the porous media [12,13].

This concept of foam injection was first introduced in 1958 by Boud and Holbrook [14]. Foam is produced when gas enters the layers of liquids that expands to enclose or trap the gas with a film of the liquid membrane [15]. The foam forms a hexagonal structure of gas cells whose cell walls consist of lamellae with approximately plane parallel sides. When three or more gas bubbles meet, the lamellae are curved by forming the plateau border [16]. There are three types of mechanisms which lead to foam generation in the porous media which are snap-off, lamella-division and leave behind [17]. The snap-off mechanism normally occurs at the pore throat area when the gas is flowing through the pore throat to the pore body. If the capillary pressure at the front is lower than the capillary pressure at the throat, this difference in capillary pressure will allow the gas bubbles to snap off [18,19]. In order for the snap off mechanism to work, the ratio of pore throat to the pore

* Corresponding author at: Department of Petroleum Engineering, Universiti Teknologi Petronas, Persiaran UTP, 32610 Seri Iskandar, Perak, Malaysia.
E-mail address: rashidah_mp@utp.edu.my (R. M. Pilus).

body must be 1 to 2.67 ratio [20]. The second mechanism for foam formation is the lamellae division. This kind of mechanism can only occur if the pre-generated foam starts to accumulate gas in the foam and forms a larger bubble size than the pore body [21]. Therefore, during the migration of gas through the pores, if the large bubble encounters a branched point and with enough capillary pressure, a division of lamellae can occur [22]. A leave-behind mechanism only occurs when there are two or more gas fronts approaching a pore body. The two fronts will converge together to form a large parallel number of lamellae [23,24].

Maintaining foams stability in the porous media under the condition of high temperature and high salinity conditions, however, prove to be quite a challenging task due to two main reasons. The first reason is that the foam strength tends to decrease with an increase of temperature. This is due to the reduction of liquid phase viscosity at higher temperatures which resulted in the liquid drainage process and the increasing rate of gas diffusion in foam lamellae [25,26]. The second reason is the limitations faced by surfactants in high temperature and high salinity conditions. This is because surfactants are known to precipitate in an aqueous media with high salinity condition due to their reaction with multivalent ions [27,28]. Moreover, some of the surfactants do not have high thermal stability and can undergo a relatively fast thermal degradation process at high-temperature condition [29]. Further to these limitations, foam stabilized by surfactants tend to have a shorter half-life in the presence of oil [30].

In recent years, nanoparticles are widely researched for oil and gas applications such as EOR, hydraulic fracturing fluids, drilling mud and wettability alteration [31–34]. In EOR applications, nanoparticles are useful in improving foam stability because the adsorbed nanoparticles help to reduce the direct contact between the fluids, therefore reducing the effect of liquid drainage, gas diffusion, and bubbles coarsening [35]. Moreover, when compared to surfactants, nanoparticles are less likely to suffer from the adsorption by reservoir rocks [36].

In spite of the advantages of nanoparticles, the application of nanoparticles for foam stabilization on a commercial scale will require another inexpensive alternative source that can be produced in large quantity for field-scale application [37]. Coal fly ash, a by-product of burning coal, can serve as a source for the low-cost large-scale production of nanoparticles [38–40]. The main factor for coal fly ash to meet is the nanoparticle's size. The importance of nanoparticle's size has been reported where the foam stability increases with the reduction of the nanoparticle's size [41]. This is because smaller nanoparticles are expected to move better in the small lamellae space between both fluids than larger-sized nanoparticles [42]. Furthermore, nanoparticle's size also affects the apparent viscosity of the foam [43]. The foam apparent viscosity and foam stability increases with decreasing nanoparticle's size because smaller nanoparticles migrate easier to the gas-liquid interface of the foam than its larger counterpart. Their movement and presence there are effective for the reduction in liquid drainage due to the high particle detachment energy presented by the nanoparticles at the interface [44]. The findings of Singh et al, the size of the fly ash particles between 18 μm and 90 μm , which is too large to be injected into the porous media, has resulted in low oil recovery [45]. The second factor is the optimal concentration of nanoparticles. Higher concentration of the nanoparticles can help reduce liquid drainage from the foam films [46]. This is because as the presence of nanoparticles at the liquid-gas interface increases with concentration, they form aggregate particles instead of a monolayer bridging particle. However, when the concentration of the nanoparticles reach its optimum point for maximum foam stability, the excess nanoparticles will agglomerate and form a larger particle network at the lamellae or at the gas-liquid interface which interferes with the formation of bubbles [47]. This is only when the concentration of nanoparticles is above the optimum concentration required, which will also affect and causes the liquid drainage to increase under the gravitational force of larger and heavier agglomerated nanoparticles [48]. This results in the liquid to start

separating from the gas bubbles leading to bubbles coalescence. Coalescence happens due to bubbles film thinning as nanoparticles, following the liquid drainage, migrate faster from the gas-liquid interface back to a liquid phase. Therefore, optimum nanoparticles concentration is required for maximum foam stability [49].

The aim of this work is divided into three parts. **The** first part is using a chemical treatment to fabricate nanoparticles from coal fly ash using both alkaline and acidic treatment instead of the conventional mechanical treatment that involves three stages: high temperature burning, wet grinding, and multiple stages of centrifugation, in order to produce a nanometer fly ash nanoparticles [45]. The second part is to investigate the effectiveness of fabricated nanoparticles on oil recovery comparing to foam without nanoparticles using static foam stability and core displacement experiments in the presence of oil. In Singh et al experiment, the foam stability of thermally treated fly ash (TTFA) nanoparticles with anionic surfactant has higher foam stability than foam without nanoparticles. However, when TTFA nanoparticles was mixed with non-ionic surfactant, the foam stability was found to be lower than that without nanoparticles. Therefore, it is important to perform static foam stability test to determine the effectiveness of nanoparticles as a foam stabilizer [45]. Furthermore, previous works have shown that the foam stability behavior may be different in and out of porous media [50,51]. The third part is to investigate the main mechanism of fabricated nanoparticles on oil recovery with foam stability.

2. Materials and methodology

2.1. Materials

Table 1 shows the chemicals and materials supplied by its respective vendors. The concentration of surfactant MFOMAX supplied by Petronas Research Sdn Bhd was 20 wt%. The surfactant is being patented hence no detailed content is provided but MFOMAX surfactant is a zwitterionic surfactant with some polymeric content in its structure [52]. The crude oil used for the experiment is taken from Baronia field located in Malaysia having a density of 0.8169 g/cm³ at 25 °C. Berea sandstone cores were used for conducting core flooding experiments in this study. The obtained Berea sandstone core samples were cylindrical in size with a diameter of 1.5 in. and a length of 6.0 in..

2.2. Preparation of fly ash nanoparticles

Firstly, the coal fly ash will be clean using acid leaching at 373.15 K with continuous stirring before undergoes the two-step chemical treatment using sulfuric acid at concentration of 10 wt%. This was done to remove any metallic impurities attached on the fly ash before the extraction of nanoparticles from fly ash. The fly ash was filtered using the Whatmann filter paper and the residue was washed with distilled water until the pH values reached seven.

Then, the leached fly ash was mixed with 2.5 M of sodium hydroxide, followed by heating at a temperature of 373.15 K for five hours. The filtrate was then mixed with 2 wt% of MFOMAX surfactant and filtered again using the Whatman filter paper. The filtrate then

Table 1
Chemicals and Materials Used.

Materials/Chemicals	Supplied By
Fly Ash	Manjung TNB power plant
Sodium Chloride	Merck Millipore
Calcium Chloride	R&M
Sodium Hydroxide	Sigma Aldrich, USA
Sulphuric Acid	Sigma Aldrich, USA
Ethanol	Thermoscientific
Whatman Filter Paper	Thermoscientific
MFOMAX surfactant	Petronas Research Sdn Bhd

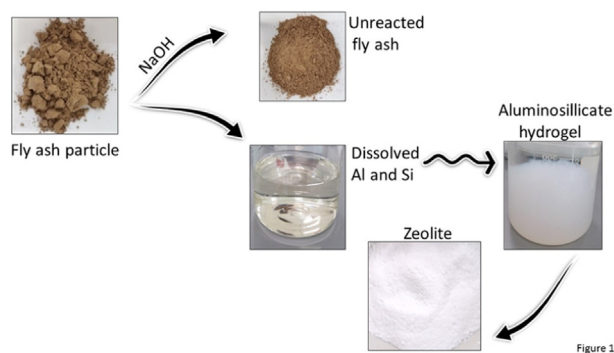


Fig. 1. Schematic Illustration of Fly Ash Chemical Treatment.

undergoes a titration process using 2.0 M of sulphuric acid with continuous stirring at the temperature of 373.15 K, until a white gel appeared which can be seen in Fig. 1 [53]. The formed gel was then aged for 24 h to get the uniform-size zeolite. The white gel was then removed and washed with distilled water and ethanol solution until the pH value was seven. The white gel was then filtered using Whatman filter paper and undergoes calcination at the temperature of 673.15 K for two hours.

2.3. Preparation of solution

After the extraction of nanoparticles from coal fly ash using chemical treatment the nanoparticles were mixed with MFOMAX solution of 0.5 wt% concentration. The MFOMAX solution also contains a salinity of 3.3 wt% salts consist of 95% NaCl and 5% CaCl₂. The nanoparticles with the MFOMAX solution will undergo mixing for 12 h using the magnetic stirrer. Followed by one to three hours of sonication using ultrasonic cleaner TPC-120, TELSONIC to stabilize nanoparticles in solution at room condition [54]. The nanoparticles used as an additive for foam injection is as described in Table 2.

2.4. Characterization of nanoparticles

The morphology of the fabricated nanoparticles and coal fly ash will be observed by Field-Emission Scanning Electron Microscope (FESEM) and the compositional elements of the fabricated nanoparticles and fly ash will be identified using Energy-Dispersive X-ray Spectroscopy (EDX). Furthermore, the chemical analysis of the fabricated nanoparticles and coal fly ash will be carried out using X-ray Photoelectron Spectrometer (XPS).

2.4.1. Static foam stability experiment

The foam stability experiment will be conducted using FoamScan® equipment from Teclis, France. A 60 ml of solution with a concentration of 10 wt% of baronia oil and different type of nanoparticles and concentration was injected into the machine. The operating condition for the experiment is set at 363.15 K for the temperature and 43.51 psi for the pressure. The injection rate was fixed at 50 cc/min. Nitrogen gas was injected at the bottom of the Foamscan® equipment through a fritted disk until the foam volume reached 150 ml. The half-life of the foam will be recorded when the foam volume falls below 75 ml. Although the morphology of the foam flowing in the porous media is

Table 2
Nanoparticles Labelling.

Nanoparticles	Description	Label
Coal Fly Ash	Coal fly ash produced from Manjung TNB, Malaysia	FA
Fabricated Nanoparticles	Nanoparticles produced from fly ash using chemical treatment	FN
MFOMAX solution without nanoparticles	MFOMAX solution without adding any nanoparticles	Base

Table 3
Concentration Ratio between MFOMAX surfactant and Nanoparticles.

Concentration	Ratio 90:10	Ratio 80:20	Ratio 70:30
MFOMAX	90	80	70
Nanoparticles	10	20	30

different from bulk foam, bulk foam stability tests are conducted as a basic screening tool to compare and evaluate foaming tendency of different chemical formulations [55,56]. Table 3 shows the three different concentration of MFOMAX surfactant and nanoparticles used in this research.

2.5. Core displacement experiment

The core displacement experiment was tested using HPHT Core Flooding System equipment from Sanchez Technologies, France. The operating parameters for temperature and pressure were fixed at 363.15 K and 1800 psi respectively. Before the experiment, the porosity of the core sample was measured using a desiccator equipment. The core is submerged into the brine solution in the desiccator equipment for one to two days under a vacuum condition. The porosity is calculated using Eq. (1) where \emptyset is porosity, W_{after} is weight of the core after submerging in the brine, W_{before} is weight of the core before submerging in the brine and ρ_{brine} is the density of the brine solution.

$$\emptyset = \frac{W_{after} - W_{before}}{\rho_{brine}} \quad (1)$$

During the core displacement experiment, the brine solution was injected into the core using three different flow rates of (0.2 cc/min, 0.5 cc/min, 1.0 cc/min) to calculate the absolute brine permeability. When the injection was at a steady state condition, the differential of inlet pressure and outlet pressure was measured, and the absolute brine permeability was calculated using equation (2) where q is the injection flow rate, A is area of the core, μ is viscosity of the brine solution, ΔP is differential pressure of inlet pressure and outlet pressure, L is length of the core and k is water permeability [57,58].

$$\frac{q\mu}{A} = k \frac{\Delta P}{L} \quad (2)$$

Baronia crude oil was then injected at a flow rate of 0.2 cc/min until no more water was produced and the initial oil saturation and the irreducible water saturation were calculated. Brine solution was injected thereafter, as primary recovery followed by nitrogen gas injection as secondary recovery. Finally, a cycle of MFOMAX solution was injected followed by nitrogen gas injection as EOR injection. All the injected solutions were injected at a flow rate of 0.2 ml/min.

2.6. History matching and sensitivity analysis

Schlumberger Eclipse 100 software was used for foam history matching from core displacement experiment. The foam model used in this work is a Local-equilibrium model, also known as "implicit texture (IT) model" [59], which does not able to clearly capture the dynamic behaviour of foam but assumes that foam creation and coalescence has reached equilibrium. This assumption is considered valid at the time-scale of a field scale applications. This model considers a non-

dimensional mobility reduction factor, FM, which is applied either to the gas phase relative permeability (k_{rg}) or its viscosity (u_g), the gas viscosity with foam is noted u_g^f as shown in equation (3) [60].

$$u_g^f = \frac{u_g}{FM} \tag{3}$$

The IT model relates the value of FM to several functions such as F_{surf} that depends on surfactant concentration, F_{dry} depending on water saturation, F_{oil} depending on oil saturation, and F_{cap} depending on the capillary number, f_{mmob} is the reference mobility factor as shown in Eq. (4) [61].

$$FM = \frac{1}{1 + f_{mmob} + F_{surf} + F_{dry} + F_{oil} + F_{cap}} \tag{4}$$

After history matching, sensitivity analysis will be done to provide a better understanding and interpretation of foam EOR. So that this result would be able to evaluate foam injection from a scale-up lab experiment to the field.

3. Result and discussion

3.1. Characterization of nanoparticles

Table 4 shows the size of the fly ash nanoparticles and fabricated nanoparticles measured by using FESEM. The size of the FA is 1 to 14 μm . After a synthesis with chemical treatment, the size of the FN was reduced to 40 to 60 nm shown. Fig. 2 shows the FESEM image of FA nanoparticles in the size of 1–14 μm [62] and Fig. 3 shows the FESEM of FN nanoparticles after chemical treatment which is in 40–60 nm.

The size reduction into the nano-material specification has proven that the two-step chemical treatment is applicable for the commercial and economic production of nanoparticles from fly ash. Unlike the ultrasound grinding or ball milling process, these two steps chemical treatment were able to reduce the synthesising process to less than a day [37]. Meanwhile, ultrasound grinding requires a two-step grinding process and an estimated 24 h to produce nanoparticles at a size of 200 nm [63].

Table 5 shows the composition of coal fly ash produced from Manjung TNB coal plant, Malaysia using EDX analysis. From the EDX analysis, the main composition of the fly ash was silicon oxide 43.26%, followed by aluminium oxide which was 20.59% and iron oxide 11.11%. The remainder of the composition was calcium carbonate and other materials in the fly ash of 3.76% and 8.79% percentage respectively. Table 6 shows the composition of fabricated nanoparticles after chemical treatment using EDX spectra. The EDX spectra confirms the presence of silicon oxide, aluminium oxide and sodium compounds in the fabricated nanoparticles. Meanwhile the elements present in the fly ash such as iron oxide, calcium carbonate and other materials were observed to be absent in the fabricated nanoparticles. The composition of the fabricated nanoparticles was 40% of silicon oxide, 59% of aluminium oxide and 1% sodium compounds. The presence of sodium compounds could be the remains of unreacted sodium silicate. This indicates the extraction of pure zeolite from fly ash.

Fig. 4 shows the chemical elements on the surface of the nanoparticles by XPS analysis. In Fig. 4, the black line represents the fly ash sample and the red line represents the FN nanoparticles. For fly ash sample, it has seven major peaks at the binding energies of 78.7, 106, 286.2, 352.3, 532.9, 7122.4 and 1072.3 eV. These peaks belong to the

Table 4
Size of nanoparticles.

Type of Nanoparticles	Size
Fly Ash	1–14 μm
Fabricated Nanoparticles	40–60 nm

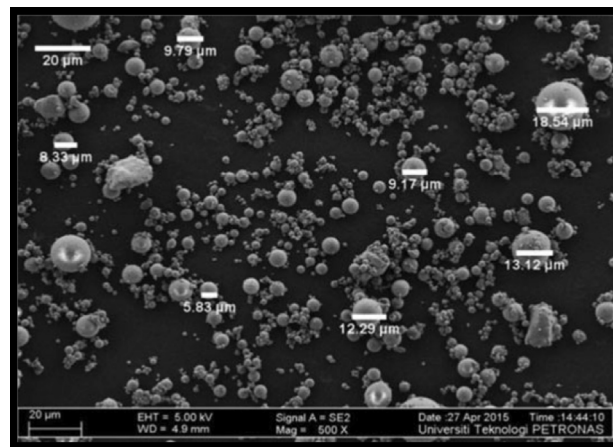


Fig. 2. FESEM image of FA nanoparticles [62].

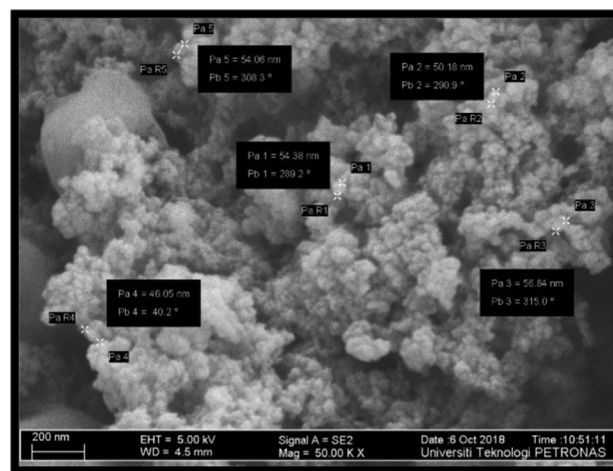


Fig. 3. FESEM image of FN nanoparticles.

Table 5
Composition of Coal Fly Ash.

Composition	Percentage
Silicon Oxide	43.26%
Aluminium Oxide	20.59%
Iron Oxide	11.11%
Calcium Carbonate	3.76%
Others	8.79%

Table 6
Composition of Fabricated Nanoparticles.

Composition	Percentage
Silicon Oxide	40%
Aluminium Oxide	59%
Sodium Compounds	1%

possible elements of aluminium, silicon, carbon, calcium, oxygen, iron and sodium elements. This indicates the presence of aluminium oxide (aluminium and oxygen elements), silicon oxide (silicon and oxygen elements), calcium carbonate (calcium, carbon and oxygen elements), iron oxide (iron and oxygen elements) and sodium compounds in the composition of fly ash. For fabricated nanoparticles, there were five major peaks at the binding energies of 74.4, 105, 532.9 and 1072 eV. These indicate the presence of elements from aluminium, silicon,

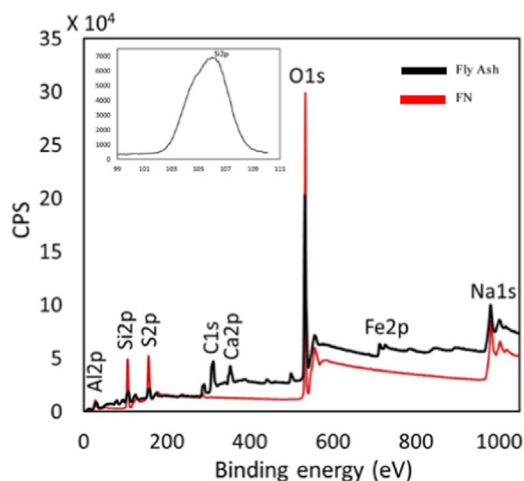
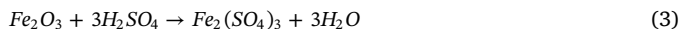
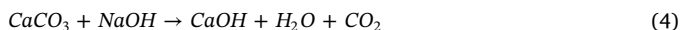


Fig. 4. XPS analyses of the fly ash and fabricated nanoparticles.

sulphur, oxygen and sodium. In fabricated nanoparticles, the presence of aluminium, silicon and oxygen elements, indicates the presence of aluminium oxide and silicon oxide. Sulphur and sodium were the dissolved ions from the solution. The fabricated nanoparticles spectra also showed the absence of iron oxide and calcium carbonate after using the two-steps chemical treatment. The iron oxide (Fe_2O_3) has reacted with the sulphuric acid (H_2SO_4) and filtered out as iron(III) sulphate ($Fe_2(SO_4)_3$) solid during washing with 10 wt% of sulphuric acid as shown in Eq. (3).



Meanwhile for calcium carbonate ($CaCO_3$), the compound was removed during alkaline treatment ($NaOH$) using sodium hydroxide to form calcium hydroxide ($CaOH$). Since calcium hydroxide is relatively insoluble in water and therefore, was filtered out as a residue using Whatmann filter paper as shown in Eq. (4)



The figure inset indicates the peak of Si 2p (refers to the Si 2p orbital of Si -1s2,2s2,2p6,3s2,3p2) obtained from fabricated nanoparticles [64].

3.2. Foam stability

There are two important parameters used to characterize foam which are foam stability and foamability. Foam stability or foam decay is the time taken for the foam volume to reach half of its initial foam volume. Fig. 5 shows the half-life of MFOMAX surfactant without nanoparticles (Base) is 400 s. Meanwhile for the fly ash sample, the half-life for the concentration of 90:10, 80:20 and 70:30 are 638 s, 738 s, and 494 s respectively. The fabricated nanoparticles (FN) half-life for the concentration of 90:10, 80:20 and 70:30 were 751 s, 875 s and 702 s. Therefore, from Fig. 5, we can conclude that surfactant with nanoparticles is able to improve foam stability regardless of the type

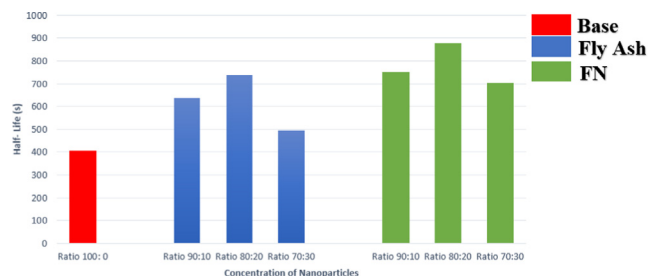


Fig. 5. Foam Stability of Nanoparticles with Different Concentration.

and concentration of nanoparticles. This is because the irreversible adsorption of the nanoparticles at the gas-liquid interface improves the foam stability by reducing the direct contact between the fluids, thus reducing the effect of liquid drainage, bubble coalescence and bubbles coarsening [64–66].

In Fig. 5, the concentration of 80:20 for fly ash sample has higher half-life compared to the concentration of 90:10 and 70:30. This was also observed in FN sample. This could be because the optimum concentration for the MFOMAX surfactant to FA or FN nanoparticles is 80:20. Normally, when the concentration of nanoparticles increases, the foam stability also increases [67] due to the increase of nanoparticles in the gas-liquid interface which helps to form an aggregate particle layer to reduce liquid drainage. However, when the concentration of nanoparticles reaches its optimum limit which is 80:20 in this experiment, the excess nanoparticles agglomerate and formed bigger particles instead. Therefore, this will reduce the number of nanoparticles in the gas-liquid interface due to its size being too large to enter the interface and leads to an increase in liquid drainage due to the increased gravitational effect on large agglomerated nanoparticles [68]. Additionally, Fig. 5 shows FN has higher foam stability than the fly ash. This is because of the larger size of the fly ash particle. The larger the size of nanoparticles, the higher the tendency for them to aggregate and causes liquid drainage. The increase in gravitational force also causes the film thinning and bubble coalescence [69].

3.3. Foamability

Foamability is measured using the time required for the foam volume to reach 150 ml. Therefore, the shorter the time required to reach 150 ml, the higher the foamability. Fig. 6 shows the foamability of MFOMAX surfactant (Base), fly ash sample and fabricated nanoparticles (FN) in MFOMAX surfactant, in three different concentrations. The foamability of the base case is at 80 s. The foamability for fly ash for the ratio of 90:10, 80:20 and 70:30 were 82 s, 81 s and 86 s. Therefore, based on the results, it shows that the fly ash sample required slightly more time to form foam especially at the 70:30 ratio. For fabricated nanoparticles, the foamability for the concentration of 90:10, 80:20 and 70:30 were 78 s, 75 s and 89 s respectively. Again, the concentration ratio of 70:30 shows longer time required for the foam to reach 150 ml foam volume compared to the other two concentrations. The findings in Fig. 6 indicates that foaming ability intends to increase when the concentration of nanoparticles increases until it reaches the optimum concentration which was 80:20. As the concentration increases to 70:30, the foamability decreases as higher time was required for the foam to generate to the required volume. Therefore, we can conclude that the presence of nanoparticles does affect foamability [70] depending on the type and concentration of nanoparticles, thus required optimization in its application. Fig. 5 shows FN has the highest foam stability followed by fly ash sample and base case as the lowest foam stability. Meanwhile in Fig. 6 FN has the highest foamability followed by base case and fly ash as the lowest in foaming ability. The fact that fly ash has lower foamability compared to the base case but in foam stability experiment the position is reversed; while FN produces the highest foamability and foam stability in both experiments, indicate

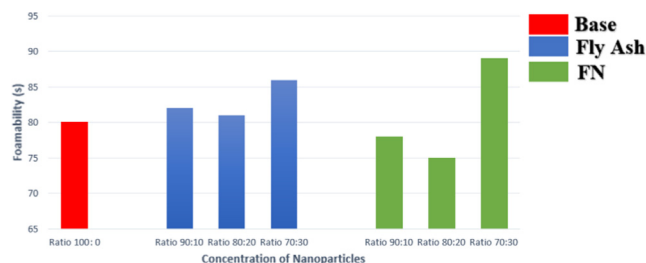


Fig. 6. Foamability of Nanoparticles with Different Concentration.

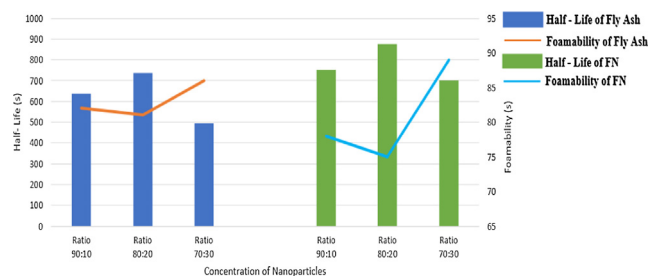


Fig. 7. Comparison of Foam Stability with Foamability.

that different nanoparticles may affect foamability and foam stability differently and that no specific trend should be reported without further studies. A similar observation has been reported by Bee Chea et al. whereby, different types of nanoparticle produced different foamability trend as compared to their foam stability trend. In their works, aluminum oxide has the highest foamability followed by silicon oxide and surfactant without nanoparticles at temperature of 363.15 K. Meanwhile in foam stability experiment, aluminum oxide has the highest foam stability followed by surfactant without nanoparticles and silicon oxide as having the lowest foam stability [71]. In addition to that, the similar result was observed by Guo et al, with the presence of nano-fly ash and without nano-fly ash, the foamability for both nanoparticles were the same at 4.5 min [72]. However, liquids with nano-fly ash has higher foam stability than liquids without nano-fly ash hence, we can deduce that in general nanoparticles that has higher foaming ability, do not necessarily produce a more stable foam.

Although there is no clear relationship between the effect of nanoparticles on foamability and foam stability in this study, there is still a clear relationship on the effect of their concentrations. Appended in Fig. 7, for both types of fly ash samples the concentration of 80:20 has the highest foamability and foam stability while the lowest is at the concentration of 70:30. The foamability is unaffected with the presence of nanoparticles at 90:10. The effect can be seen only at the higher concentration unlike stability. Thus, we can conclude that generally the foamability and foam stability increases as the concentration of nanoparticles increases until it reaches optimum concentration [73–75].

3.4. Oil recovery

Based on the bulk foam stability screening test, fabricated nanoparticle with a concentration of 80:20 which has the highest foam stability was chosen for the core displacement experiment. Table 7 shows the results of oil recovery on water injection, gas injection, and SAG injection using MFOMAX with and without FN nanoparticles. In the application of SAG injection, the oil recovery for the base case is 4.96%. Meanwhile, the oil recovery for FN nanoparticles in SAG injection is 5.22%.

The increment of oil recovery by FN nanoparticles is acceptable to prove the technique's ability to recover residual oil. The objective of foam injection as an EOR method is to further reduce the residual oil saturation, which is normally a very small volume in the porous media. The similar result observed in the work of Singh et al. for the

Table 7

Oil Recovery Comparison of Base Case and FN Case.

Core Sample Code		1	2
		Base	FN
The ratio of surfactant/Nanoparticles		100:0	80:20
Nanoparticles concentration (wt%)		0	0.125
Water Injection	Oil Recovery (%)	34.38	31.42
Gas Injection	Oil Recovery (%)	18.62	17.70
Water and Gas Injection	Total Oil Recovery (%)	53.0	49.12
SAG Injection	Oil Recovery (%)	4.96	5.22
Water, Gas and SAG Injection	Final Oil Recovery (%)	57.96	54.34

comparison of residual oil recovery by foam with and without nanoparticles where an increase of 1.3% of residual oil reported. This is a reliable indication for an 8 to 10 PV of nitrogen foam injection into a Berea core with a size of 0.6-inch diameter and 6.0-inch length [76]. Additionally, for a homogeneous core of less than one inch in diameter, there was no scope to improve the volumetric sweep efficiency. Risal et al shows a similar oil recovery increment using the glass-bead pack core displacement experiment. The result of oil recovery for foam without silica nanoparticles, foam with silica nanoparticles and foam with modified silica (surface hydrolyzed to 60% Si-OH, purity > 96.3%) were 0.63%, 0.67% and 0.73% respectively. [77].

Although nanoparticles retention is not measured in this core displacement experiment, we believe that nanoparticles retention may not be an important phenomena as based on the previous works of Singh et al, where 99.57% of the nanoparticles used for injection were recovered with the remaining of less than 1% retained in the porous media [76]. Murphy et al reported that the nanoparticles recovery from injection were 95% and 96% for two different type of coated silica nanoparticles [78]. Therefore, we believe that foam stability, and may be surfactant adsorption, were the influencing factor on the oil recovery observed rather than nanoparticles retention in this experiment.

3.5. Mobility reduction factor (MRF) for base case

The performance of foam is important to evaluate the effectiveness of nanoparticles during foam flooding application. The performance of foam can be measured through mobility reduction factor (MRF) which is defined as the pressure drop across the core with foam flow divided by the pressure drop across the core without foam. The MRF value is higher than one indicates the presence of foam in the core and a much higher MRF value indicates a much stronger foam which able to stabilize the gas front and delaying the gas breakthrough. Fig. 8 shows the MRF value of the MFOMAX foam without nanoparticles (Base Case), and the MRF value was higher than one throughout the FAWAG injection. This indicates that there was the presence of foam throughout the injection and across the core

3.6. Mobility reduction factor (MRF) for FN nanoparticles

Fig. 9 shows the mobility reduction factor (MRF) of FN nanoparticles with MFOMAX surfactant. The MRF value increases initially during the SAG injection. However, after injecting more than 10 ml, the MRF value drop below one which indicates no foam in the core during the 10 ml of total injection. MRF value starts to increase again at the 14 ml of total injection. This indicates the foam decaying and foam regenerating process during surfactant alternating gas (SAG) injection. Further injection, from 15 ml of total injection onwards to the end of SAG injection also showed a similar trend where MRF increases higher than the value of 4 and decreases to less than one. The instability of the MRF values indicates the instability of the foam to provide more resistance to nitrogen gas to flow in the porous media. This is because the foam was weakened by the oil droplets flowing into the foam lamellae [79]. The higher the concentration of the oil droplets flowing in the foam lamellae, the higher the chance for the foam to collapse. After the total volume of injection of 189 ml, the MRF value were much lower compared with the previous pore volume. This was because the foam quality decreases at this stage. The higher the MRF value, indicates higher apparent viscosity [80] which translates into a higher foam apparent viscosity, a higher foam quality [81]. With a higher foam quality, a higher volume of gas was trapped in the foam. Therefore, a higher MRF value in foam with FN nanoparticles indicates that a higher volume of gas trapped in the foam than in the base case.

3.7. Gas breakthrough

Fig. 10 shows the total gas collected when surfactant alternating gas

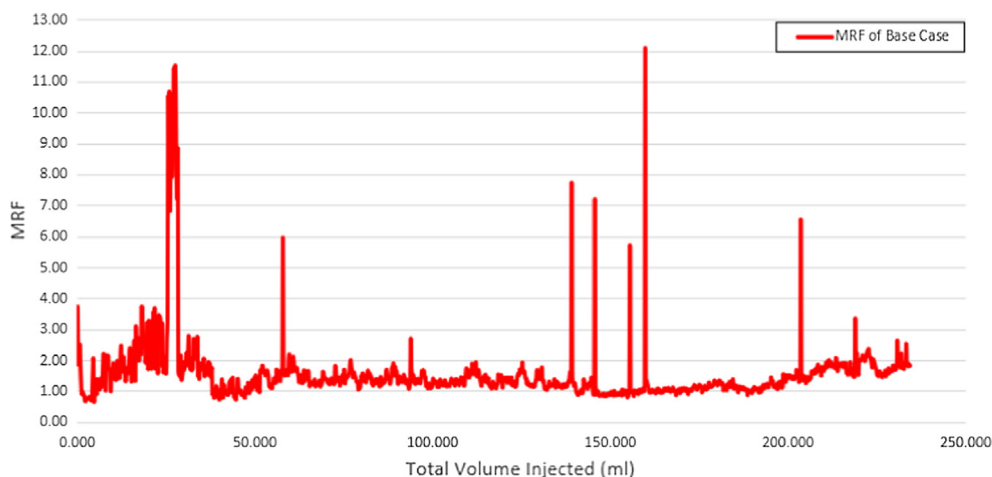


Fig. 8. MRF value of Base Case (MFOMAX surfactant without nanoparticles).

(SAG) injecting into the core. At 15.7 ml of SAG injection, the total gas collected increases to 950 ml from 148.2 ml. This indicates the first gas breakthrough for the base case. However, the MFOMAX foam without nanoparticles (Base Case) shows a straight line after the gas breakthrough. This indicates foams were regenerating from the SAG injection. The graph shows a steady straight line throughout the injection which indicates that the base case has good foam stability within that duration. Thus, it can conclude that MFOMAX surfactant has good foam stability in high temperature and high-pressure condition as this experiment was carried out at 363.15 K temperature and 1800 psi pressure stated earlier. For fabricated nanoparticles (FN), it has a slower first gas breakthrough than the base case which is at 18.8 ml. However, from 18.8 ml onwards, the gas collected keep increasing at a steady state until it reaches 144.6 of total gas collected. These observations highlight 2 important findings: firstly, the FN does not form a more stable foam as compared to the surfactant alone in porous media although the result in bulk foam test indicated otherwise. Secondly, although the base case which was surfactant alone, showed a higher foam stability in the core displacement experiment, the oil recovery from surfactant foam was lower from the foam with FN nanoparticles in Table 7. These indicates that there are other factors in the reservoir that can affect oil recovery other than just improving the stability of foam thus controlling the gas mobility as explained in the next paragraph. These other factors could be attributed to capillary pressure and wettability of the rock.

The fact that foam with FN nanoparticles was unstable could also

mean the foam was actually carrying higher oil saturation in the foam than the base case. When the foam is carrying higher oil saturation, the foam tends to be unstable with the increasing oil saturation slipping into lamellas. The foam will completely collapse when the saturation of oil in the foam reaching beyond critical foaming oil saturation [82]. This justified our findings that the oil recovered by the foam with FN nanoparticles, which foam was more unstable, was higher than the base case. This also indicate that in improving the stability of foam, so that it could sweep out more oil, the technique should focus on increasing the critical foaming oil saturation capability of the foams. This and other factors such as capillary pressure, wettability of the rock, and capillary number could be mutually contributing to higher oil recovery [83].

3.8. History matching

Based on the result of the core displacement experiment, fabricated nanoparticles with MFOMAX surfactant (Experimental) was chosen for history matching and sensitivity analysis because it recovered more oil than MFOMAX surfactant without nanoparticles. In Table 8, the total oil collected from water injection, gas injection and foam injection are 31.42%, 17.70% and 5.22% respectively. While in the simulation run, the total oil recovery for water injection, gas injection and foam injection are expected to be 33.65%, 15.70% and 5.14%. The percentage difference between experimental and simulation results for water injection is 2.23%, 2.00% and 0.08%. In simulation history matching for water injection, the oil recovery percentage is 2.23% higher than the

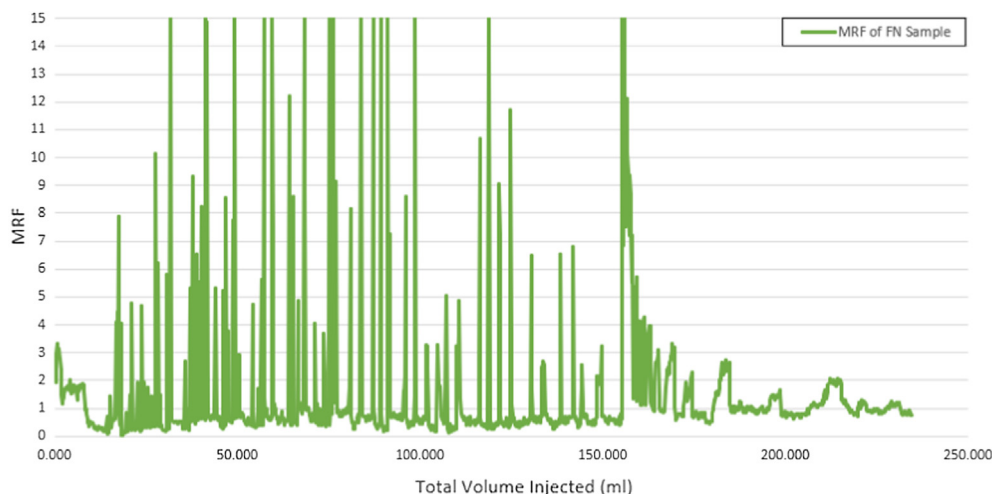


Fig. 9. MRF value of Fabricated Nanoparticles (FN) Case.

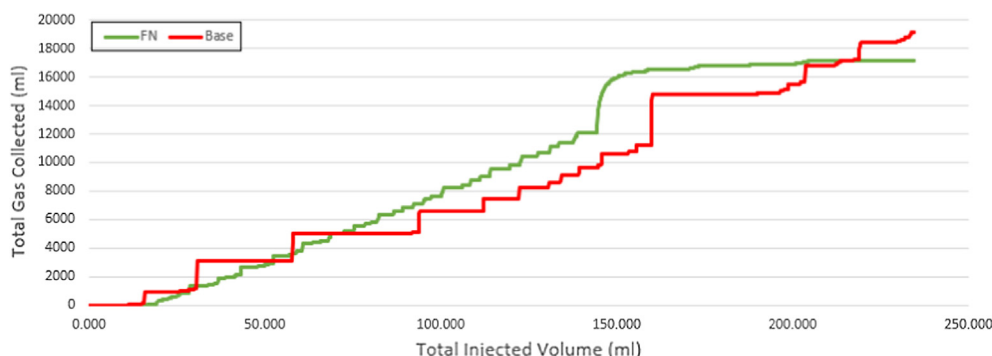


Fig. 10. Graph of Total Gas Injected vs Total Gas Collected.

Table 8
Oil Recovery Comparison between Experimental and Simulation Run.

Oil Recovery Percentage (%)	Experimental	Simulation
Total Oil recovery by Water injection	31.42%	33.65%
Total Oil recovery by Gas injection	17.70%	15.70%
Total Oil by Foam injection	5.22%	5.14%
Final Oil Recovery (Water + Gas + Foam Injection)	54.34%	54.49%

Table 9
Pore Volume of the Core in Experiment.

Total Pore Volume of Core	38.28 cc
Total Pore Volume of Water in Core	15.68 cc
Total Pore Volume of Oil in Core	15.50 cc
Total Occupied Space in Core (Total Pore Volume of Water + Oil in Core)	15.68 cc + 15.50 cc = 31.18 cc
Total Empty Space in Core (Total Pore Volume - Total Occupied Space in Core)	38.28 cc - 31.18 cc = 7.1 cc

experimental result. This may be due to the empty space in the core that does not contain water or oil in the pore as shown in table 9. The empty pore or better known as pore space are in-effective pores in the core. The empty pore may have a channel that has only narrow single connection to the other interconnected pore space or just an isolated pore with no connectivity [84]. Therefore, the percentage error in the simulation would be higher than normal due to the assumption made in the simulation whereby the 7.1 cc empty space in the core was predicted to be occupied by water instead and this may result in a higher boost of oil recovery than the original oil collected from the experiment [85]. The percentage of oil recovery difference for gas injection and foam injection for simulation history match is about 2.00% and 0.08% respectively. Both injections show that the oil recovery percentage is slightly lower than the original experiment.

These are the various assumptions made in simulation compared to experiment:

1. The porous media is assumed in three phases

2. The flow in all the injections are considered in steady state
3. Surfactant alternating gas injection is assumed as co-injection of foam into the porous media
4. The simulator does not model foam generation in the porous media
5. Gas, oil and water are presented in the beginning of the simulation, purpose to enable the foam model in the simulation
6. The reservoir has isotropic and uniform permeability and porosity
7. The injection is assumed to be in a cylindrical geometry for a rectangular shaped grid block, and uniform properties in the grid block.
8. The presence of C1 to C4 hydrocarbons are present in the simulation model meanwhile in the experiment, C1 to C4 hydrocarbon is absent in the Baronia oil content for experiment

Table 10 shows the comparison between oil recovery in experiments and history matching simulation run. The oil recovery by an experimental run for water injection, gas injection and foam injection were 4.8701 cc, 2.7435 cc and 0.8091 cc respectively whereas for simulation run was 4.428 cc for water injection, 2.068 cc for gas injection and 0.684 cc for foam injection. In all different injection scenario, the actual oil recovery predicted by simulation run was lower than the experimental run. This may be due to the presence of gas in the pore volume being produced along with the oil in the simulation. The presence of gas in the pore volumes was needed for the simulation model to enable injection of foam and gas in the model. Water injection shows the lowest percentage error compared to other injections which was 9.08% when compared with the experimental run. Gas injection in the simulation shows the highest percentage error compared to the experiment which is 24.62%. Foam injection shows a slightly lower percentage error compared to gas injection and a higher percentage error compared to water injection which is 15.46%. Overall, the final oil recovery of the simulation has an error of 14.75% when compared with the experimental run. These observations were due to reservoir heterogeneity, capillary pressure and relative permeability between simulation and experiment, and experiment flow measurement errors [86]. According to Saleri et al, hydrocarbon cumulative production accuracies in the simulation would tend to be in range of 10% to 40%. Availability of reservoir and production history information can push

Table 10
Oil Production Rate of Experiment Run and Simulation Run.

Oil Recovery	Experiment	Simulation
Water Injection	4.8701 cc	4.428 cc
Gas Injection	2.7435 cc	2.068 cc
Gas and Water Injection	7.6136 cc	6.496 cc
Foam Injection	0.8091 cc	0.684 cc
Final Oil Recovery (Water + Gas + Foam Injection)	8.4227 cc	7.179 cc
Percentage Difference, cc (%) [Comparison of Experiment and Simulation]		
	Water Injection	0.4421 cc (9.08%)
	Gas Injection	0.6755 cc (24.62%)
	Foam Injection	0.1251 cc (15.46%)
	Final Oil Recovery	1.2427 cc (14.75%)

the forecasts to the lower end of the spectrum. However, accuracies below 10% are more likely to be artifacts of compensating errors or luck than precise engineering or geology [87].

3.9. Sensitivity analysis of surfactant adsorption

Sensitivity analysis is done using the history matching foam injection simulation model and Eq. (2) to determine major influence of foam in oil recovery. According to Eq. (2), FM or Foam Mobility is depending on surfactant concentration (F_{surf}), water saturation (F_{dtp}), oil saturation (F_{oil}), capillary number (F_{cap}) and mobility reference factor (f_{mmob}). However, in this simulation water saturation, capillary number and reference factor have been defaulted. Since the Berea core is a horizontal homogenous permeability core, one of the foam functions which is “plugging the high permeability” was neglected. Therefore, the half-life of foam on water saturation was not taken. In this simulation model, the capillary number was calculated using the concentration of foam against surface tension, and since the experiment was unable to measure this value, the data was put constant according to the Eclipse 100 software. The effect of surfactant concentration was model based on adsorption of the core and the maximum concentration of the surfactant was 0.5 wt% which was the concentration of surfactant injected. For oil saturation, the static foam stability data was used to model the foam. This is because the core displacement equipment could not measure dynamic foam stability. Therefore, this could be the main contributor to the large error of 15.46% of oil recovery between experiment and simulation run.

Sensitivity analysis will be done to provide a better understanding and interpretation of foam EOR so that future research can focus on reducing surfactant adsorption or increasing foam stability for the application of this synthesized surfactant, for better oil recovery. Fig. 11 shows the oil recovery of surfactants and their different adsorption rates. HS is referred to foam history matching model based on core displacement experiment using surfactant with fabricated nanoparticles in Table 10. HS with -25% is the history match foam model with surfactant adsorption by the reservoir rock was reduced by 25% followed by HS with -50% and -75%, when the adsorption was reduced by 50% and 75% respectively. The oil recovery for foam injection in HS was 0.684 cc from Table 10. HS with -25%, -50%, and -75%, have shown 0.72 cc, 0.79 cc, and 0.89 cc of oil recovery respectively. Although the volume of oil recovered for three different adsorption rate was still less than 1.00 cc, in terms of percentage difference, it was high between the varying adsorption rates: 5.84%, 15.75% and 30.69% for the HS with -25%, -50% and -75% respectively. Therefore, it can be concluded that when the surfactant adsorbed onto the rock decreases, the oil recovery will increase.

3.10. Sensitivity analysis for half-life of foam

Fig. 12 indicates the oil recovery by the different foam stability in

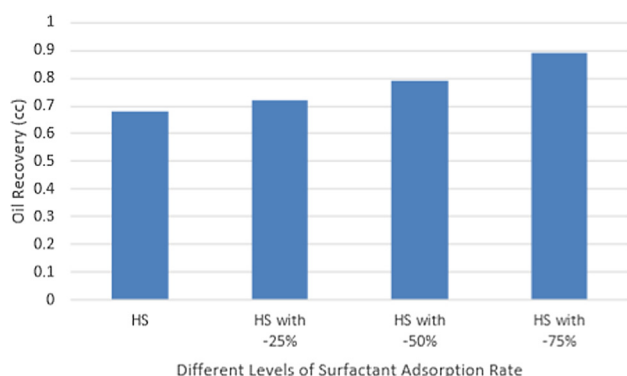


Fig. 11. Oil Recovery for Different Levels of Surfactant Adsorption Rate.

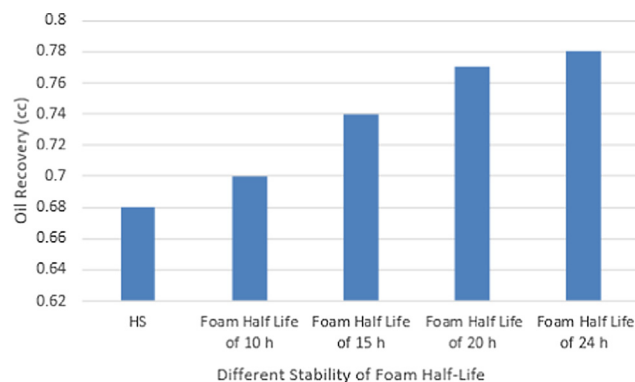


Fig. 12. Oil Recovery Comparison with Different Stability of Foam Half-Life.

the presence of oil. The value for oil saturation (F_{oil}) was changed to 10 h, 15 h, 20 h and 24 h of foam half-life model. HS is referred to foam history matching model based on core displacement experiment using surfactant with fabricated nanoparticles. The graph shows an increasing trend of oil recovery starting from HS, foam half-life of 10 h up to 24 h as expected. The oil recovered from HS was 0.684 cc. Meanwhile, for HS with foam half-life of 10 h, and continuous additional of about 5 h in half-life were 0.70 cc, 0.74 cc, 0.77 cc and 0.78 cc respectively. Other than increase in volume, the oil recovery percentage difference when compared to HS for the half-life of 10 h, 15 h, 20 h and 24 h is 2.34%, 8.19%, 12.57% and 14.04% respectively. According to the sensitivity analysis of half-life of foam, although the foam was extended longer to 24 h, the increment of oil recovery predicted was almost 15% from HS oil recovery. Meanwhile, in section 4.9 the increment of oil recovery for surfactant adsorption was 30.69% when the surfactant adsorption was reduced by 75%. However, the oil recovery was only half of this value when the foam half-life was 24 h. This is because to achieve the maximum oil recovery by adjusting the foam half-life, an optimum half-life has to be met. Should the foam half-life be extended beyond this optimum limit, the oil recovery improvement will reach a plateau [88]. Furthermore, we believe that when the foam half-life reaches the 20 h, the foam half-life is at the optimum limit. This is because the oil recovery improvement has reached a plateau level when the foam half-life increases from 20 h to 24 h. This can be seen by comparing the oil recovery between the foam half-life of HS with 10 h, 10 h with 15 h, 15 h with 20 h and 20 h with 24 h were 0.016 cc, 0.04 cc, 0.03 cc and 0.01 cc respectively. The oil recovery improvement of the foam half-life of 20 h increases up to 24 h has lowest oil recovery improvement. As a conclusion, the optimum half-life would be required to generate the maximum oil recovery and, in this case, 20 h of foam half-life is the optimum limit.

4. Conclusion

The utilization of two-step chemical treatment has successfully produced nanoparticles with a size less than 100 nm. The size of the fabricated nanoparticles was 40 nm to 60 nm and the composition of FN nanoparticles were mainly silicon oxide and aluminium oxide with 1% sodium compounds. Static foam stability experiment at reservoir conditions was performed to investigate the effect of nanoparticles as an additive in foam stability and foamability. It was also a screening tool to select the best type of nanoparticles and concentration ratio for surfactant/nanoparticles formulation for further application in porous media i.e. the core flooding experiments. The results from the static foam experiments showed that the nanoparticles have the potential of an additive to increase foam stability with the MFOMAX surfactant. Of all the mixture ratio tested, the highest performance for foam stability and foamability was fabricated nanoparticles at a ratio of 80:20. At the 80:20 concentration, the foam was stronger and remain stable for

generally twice the time achieved with MFOMAX surfactant alone. The foamability of 80:20 concentration was highest among others. Therefore, from the bulk foam stability experiment, we can conclude that the foamability and foam stability increases as the concentration of nanoparticles increases until it reaches an optimum concentration. In the core displacement experiments conducted at reservoir conditions of 363.15 K and 1800 psi, the residual oil recovery was higher with the presence of FN nanoparticles as compared to surfactant foam without it with an increment of 0.26%. In the use of FN nanoparticles as an additive, the MRF value was increased upon SAG injection with an average value of 4 as compared to the base case of 2. The higher MRF value indicates a higher foam apparent viscosity which translates into a higher foam quality. A higher foam quality indicates a higher gas volume stored in the foam. On the other hand, the MRF value of base case is more stable compared to the MRF value with FN nanoparticles because the instability of MRF values with FN nanoparticles because foam with FN nanoparticles is believed to be carried higher oil saturation than base case. The MRF value of base case shown in Fig. 8 has less fluctuation at a average value of 1.3. Meanwhile, MRF value of FN shown in Fig. 9 has more fluctuation lines from less than 1 and increase up to 15. This highlights the importance to realise that the foam stability does not necessarily brings about a higher oil recovery. The instability of the MRF values indicates the instability of the foam due to the foam being weakened by the oil droplets flowing into the foam lamellae. The higher the concentration of the oil droplets in the foam lamellae, the higher the chance for the foam stability to decrease or foam collapse. Furthermore, the foam with FN nanoparticles has higher MRF value of above 15 than base case which has MRF value of 12. The core displacement also showed a faster gas breakthrough by foam without nanoparticles compared to foam with FN nanoparticles. However, foam of the base case has a steadier increase of volume of gas and a smaller number of times for gas breakthrough compared to foam with FN nanoparticles. This indicates that foam with FN nanoparticles is actually carrying higher oil saturation in the foam lamellae than base case because foam tends to be unstable with the increasing of oil saturation. The simulation history matching, and sensitivity analysis were performed to investigate the major influence on oil recovery by the foam. History matching was done to validate the reservoir simulation model and to adjust the model until it closely reproduces the behaviour of the core displacement experiment. Overall, the history matching process of the simulation model has a 14.87% oil production with the highest oil production percentage error coming from gas injection and foam injection. This because of the presence of gas in the porous media beginning of the simulation and the purpose gas is present in the beginning was part of the simulator requirement for foam injection model, and the presence of C1 to C4 in the hydrocarbon to produce natural gas in the simulator meanwhile in the experiment, the hydrocarbon of C1 to C4 are absence. In the sensitivity analysis, two major influence of foam on oil recovery were investigated which were surfactant adsorption and foam half-life. Owing to the fact that the increment of oil recovery by reducing the surfactant adsorption of 75% was 30.69% and oil recovery from foam stability with a half-life of 24 h was only 14.04% increment, we can conclude that in the application of MFOMAX surfactant for fabricated nanoparticles foam. surfactant adsorption reduction may become a main factor to focus on besides increasing the stability of foam.

CRedit authorship contribution statement

Guan Ming Phong: Investigation, Software, Validation, Writing - original draft, Writing - review & editing. **Rashidah M. Pilus:** Writing - review & editing, Supervision, Resources, Conceptualization, Methodology. **Afiq Mustafa:** Investigation. **Lakshmi Priya Thangavel:** Investigation, Resources, Methodology. **Norani Muti Mohamed:** Conceptualization, Supervision.

Declaration of Competing Interest

The authors declare that they have no known competing financial interests or personal relationships that could have appeared to influence the work reported in this paper.

Acknowledgements

The author would like to acknowledge the Center of Research in Enhanced Oil Recovery (COREOR), Universiti Teknologi Petronas for providing technical facilities. And gratitude to the TU Delft—SHELL—UTP—Petronas project (0153 AB-DA8) for the financial assistance.

References

- [1] Franklin J, Orr M. Theory of gas injection processes. Copenhagen, Denmark: Tie-Line Publications; 2007.
- [2] Christensen JR, Stenby EH, Skauge A. Review of WAG field experience (SPE 71203). SPE Reserv Eval Eng 2001;4(2):97–106.
- [3] Rao D. Gas injection EOR - a new meaning in the new millennium. J Can Pet Technol 2001;40(2):11–9.
- [4] Stalkup FI. Status of Miscible Displacement (SPE 9992). JPT J Pet Technol 1983;35(4):815–26.
- [5] Green Don W, Paul Willhite G. Enhanced Oil Recovery. Society of Petroleum Engineers; 1998.
- [6] Lake LW. Enhanced oil recovery. Englewood Cliffs: Prentice-Hall Inc.; 1989.
- [7] Lake LW, Johns Russell T, Rossen WR, Pope GA. Fundamentals of enhanced oil recovery. Society of Petroleum Engineers; 2014.
- [8] Wang S, Chen C, Kadum MJ, Shiao BJ, Harwell JH. Enhancing foam stability in porous media by applying nanoparticles. J Dispers Sci Technol 2018;39(5):734–43.
- [9] Horjen HT. CO₂ Foam stabilization with nanoparticles and EOR in fractured carbonate systems Master Thesis Department of Physics and Technology, University of Bergen; 2015
- [10] Rossen WR. Foam in porous media. In: Sadoc JF, Rivier N, editors. Foams and Emulsions, NSSE, Volu. Dordrecht: Springer; 1999. p. 335–48.
- [11] Smith DH. Foams: fundamentals and applications in the petroleum industry. Washington, DC: American Chemical Society; 1994.
- [12] Tang GQ, Kovscek AR. Trapped gas fraction during steady-state foam flow. Trans Porous Media 2006;65(2):287–307.
- [13] Skauge A, Aarra MG, Surguchev L, Martinsen HA, Rasmussen L. Foam-Assisted WAG: experience from the Snorre Field (SPE 75157). SPE/DOE Improved Oil Recovery Symposium. 2002.
- [14] Bond DC, Holbrook OC, Lake C. "Gas Drive Oil Recovery Process," US2866507A.
- [15] Krause JP. "Foams. Theory, Measurements, and Applications. Edited by R. K. Prud'homme and S. A. Khan. VIII and 596 pages, numerous figures and tables. Marcel Dekker, Inc., New York, Basel, Hong Kong 1996. Price: 165.75 US \$.," Food/Nahrung, vol. 41, no. 1, pp. 55–55, 1997.
- [16] Falls AH, Hirasaki GJ, Patzek TW, Gauglitz DA, Miller DD, Ratulowski T. "Development of a mechanistic foam simulator: the population balance and generation by snap-off (SPE 14961). SPE Reserv. Eng. (Society Pet. Eng.) 1988;3(3):884–92.
- [17] Vasshus S. Experimental study of foam generation and flow in carbonate fracture systems Master Thesis Department of Physics and Technology, University of Bergen; 2016
- [18] Morin B, Liu Y, Alvarado V, Oakey J. A microfluidic flow focusing platform to screen the evolution of crude oil-brine interfacial elasticity. Lab Chip 2016;16(16):3074–81.
- [19] Roof G. Snap-off of oil droplets in water-wet pores (SPE 2504). Soc Pet Eng J 1970;10(1):85–90.
- [20] Kovscek AR, Radke CJ. Fundamentals of foam transport in porous media. In: Schramm LL, editor. Foams: Fundamentals and Applications in the Petroleum Industry. 1994. p. 115–63.
- [21] Li B, Hirasaki GJ, Miller CA. Upscaling of foam mobility control to three dimensions (SPE 99719). SPE/DOE Symposium on Improved Oil Recovery. 2006.
- [22] Ransohoff TC, Radke CJ. Mechanisms of foam generation in glass-bead packs (SPE 15441). SPE Reserv Eng 1989;3(2):573–85.
- [23] Chen M, Yortsos YC, Rossen WR. A pore-network study of the mechanisms of foam generation (SPE 90939). Proc. - SPE Annu. Tech. Conf. Exhib. 2004. p. 4393–412.
- [24] Mannhardt K, Novosad JJ, Schramm LL. Foam/oil interactions at reservoir conditions. SPE/DOE improved oil recovery symposium. 1998.
- [25] Israelachvili JN. Intermolecular and surface forces. San Diego, Calif: Academic Press; 2011.
- [26] Yang W, Wang T, Fan Z. Highly stable foam stabilized by alumina nanoparticles for EOR: effects of sodium cumenesulfonate and electrolyte concentrations. Energy Fuels 2017;31(9):9016–25.
- [27] Stellner KL, Scamehorn JF. Surfactant precipitation in aqueous solutions containing mixtures of anionic and nonionic surfactants. J Am Oil Chem Soc 1986;63(4):566–74.
- [28] Amante JC, Scamehorn JF, Harwell JH. Precipitation of mixtures of anionic and cationic surfactants. II. Effect of surfactant structure, temperature, and pH. J Colloid

- Interface Sci 1991;144(1):243–53.
- [29] Handy LL, Amaefule JO, Ziegler VM, Ershaghi I. SPE 7867 Thermal Stability of Surfactants for Reservoir Application (includes associated papers 11323 and 11597). Soc Pet Eng J 1982;22(05):722–30.
- [30] Farajzadeh R, Andrianov A, Krastev R, Rossen WR, Hirasaki GJ. Foam-oil interaction in porous media-Implications for foam-assisted enhanced oil recovery (SPE 154197). 74th Eur. Assoc. Geosci. Eng. Conf. Exhib. 2012. Int. SPE Eur. 2012. Responsibly Secur. Nat. Resour. 2012. p. 4996–5016.
- [31] Emrani AS, Ibrahim AF, Nasr-El-din HA. Evaluation of mobility control with nanoparticle-stabilized CO₂ foam (SPE 185551). SPE Lat. Am. Caribb. Pet. Eng. Conf. Proc. 2017. p. 18–9.
- [32] Barati R, Johnson SJ, McCool S, Green DW, Willhite GP, Liang J-T. Polyelectrolyte complex nanoparticles for protection and delayed release of enzymes in alkaline pH and at elevated temperature during hydraulic fracturing of oil wells. J Appl Polym Sci 2012;126(2):587–92.
- [33] Zakaria MF, Husein M, Hareland G. Novel nanoparticle-based drilling fluid with improved characteristics (SPE 156992). Soc. Pet. Eng. - SPE Int. Oilf. Nanotechnol. Conf. 2012. p. 232–7.
- [34] Karimi A, et al. Wettability alteration in carbonates using zirconium oxide nanofluids: EOR implications. Energy Fuels 2012;26(2):1028–36.
- [35] Khajepour M, Reza Etminan S, Goldman J, Wassmuth F. Nanoparticles as foam stabilizer for steam-foam process (SPE 179826). Society of Petroleum Engineers - SPE EOR Conference at Oil and Gas West Asia, OGWA. 2016.
- [36] Karakashev SI, Ozdemir O, Hampton MA, Nguyen AV. Formation and stability of foams stabilized by fine particles with similar size, contact angle and different shapes. Colloids Surf A Physicochem Eng Asp 2011;382(1–3):132–8.
- [37] Lee D, Cho H, Lee J, Huh C, Mohanty K. Fly ash nanoparticles as a CO₂ foam stabilizer. Powder Technol Oct. 2015;283:77–84.
- [38] Singh R, Mohanty KK. Nanoparticle-stabilized foams for high-temperature, high-salinity oil reservoirs (SPE 187165). Proc. - SPE Annu. Tech. Conf. Exhib. 2017.
- [39] Huh C, Cho H. Silica, fly ash and magnetite nanoparticles for improved oil and gas production. Korean Soc Miner Energy Resour Eng 2018;55(4):272–84.
- [40] Ahmad I, Awang MB, Mumtaz M, Noor MZM. Development and evaluation of fly ash particle for foam stability for possible application to foam flooding. J Sci Res Dev 2015;2(14):166–71.
- [41] Tang FQ, Xiao Z, Tang JA, Jiang L. The effect of SiO₂ particles upon stabilization of foam. J Colloid Interface Sci 1989;131(2):498–502.
- [42] Deleurence R, Parneix C, Monteux C. Mixtures of latex particles and the surfactant of opposite charge used as interface stabilizers-influence of particle contact angle, zeta potential, flocculation and shear energy. Soft Matter 2014;10(36):7088–95.
- [43] Kim I, Worthen AJ, Johnston KP, DiCarlo DA, Huh C. Size-dependent properties of silica nanoparticles for Pickering stabilization of emulsions and foams. J Nanopart Res 2016;18(4).
- [44] Stocco A, Rio E, Binks BP, Langevin D. Aqueous foams stabilized solely by particles. Soft Matter 2011;7(4):1260–7.
- [45] Singh R, Gupta A, Mohanty KK, Huh C, Lee D, Cho H. Fly ash nanoparticle-stabilized CO₂-in-water foams for gas mobility control applications (SPE 175057). Proceedings - SPE Annual Technical Conference and Exhibition. 2015. p. 4815–27.
- [46] Carn F, Colin A, Pitois O, Vignes-Adler M, Backov R. Foam drainage in the presence of nanoparticle-surfactant mixtures. Langmuir 2009;25(14):7847–56.
- [47] AlYousef Z, Almorbarky M, Schechter D. Enhancing the stability of foam by the use of nanoparticles. Energy Fuels 2017;31(10):10620–7.
- [48] Li Z, Liu Z, Li B, Li S, Sun Q, Wang S. Aqueous foams stabilized with particles and surfactants (SPE 160840). Society of Petroleum Engineers - SPE Saudi Arabia Section Technical Symposium and Exhibition 2012. 2012. p. 61–9.
- [49] Eftekhari AA, Krastev R, Farajzadeh R. Foam stabilized by fly ash nanoparticles for enhancing oil recovery. Ind Eng Chem Res 2015;54(50):12482–91.
- [50] Farajzadeh R, Andrianov A, Krastev R, Hirasaki GJ, Rossen WR. Foam-oil interaction in porous media: Implications for foam assisted enhanced oil recovery. Advances in Colloid and Interface Science, vol. 183–184. Elsevier B.V.; 2012. p. 1–13.
- [51] Tang J, Vincent-Bonnieu S, Rossen WR. CT coreflood study of foam flow for enhanced oil recovery: the effect of oil type and saturation. Energy 2019;188.
- [52] Hanamertani AS, Pilus RM, Manan NA, Mutalib MIA. The use of ionic liquids as additive to stabilize surfactant foam for mobility control application. J Pet Sci Eng 2018;167:192–201.
- [53] Lakshmi Priya T, Mohamed N, Bashiri R, Pilus RM, Mustafa A. Extraction of zeolite nanoparticles from industrial waste of coal fly ash by alkali reduction. Conf Appl Surf Sci 2019.
- [54] Sun Q, Zhang N, Li Z, Wang Y. Nanoparticle-stabilized foam for mobility control in enhanced oil recovery. Energy Technol 2016;4(9):1084–96.
- [55] Singh R, Mohanty KK. Foams with wettability-altering capabilities for oil-wet carbonates: a synergistic approach (SPE 175027). Proc. - SPE Annu. Tech. Conf. Exhib. 2015. p. 4372–94.
- [56] Hadian Nasr N, Mahmood SM, Hematpur H. A rigorous approach to analyze bulk and coreflood foam screening tests. J Pet Explor Prod Technol 2019;9(2):809–22.
- [57] Hanamertani AS, Pilus RM, Manan NA, Ahmed S, Awang M. Ionic liquid application in surfactant foam stabilization for gas mobility control. Energy Fuels 2018;32(6):6545–56.
- [58] Rezk MG, Foroozesh J, Zivar D, Mumtaz M. CO₂ storage potential during CO₂ enhanced oil recovery in sandstone reservoirs. J Nat Gas Sci Eng 2019:233–43.
- [59] Farajzadeh R, Lotfollahi M, Eftekhari AA, Rossen WR, Hirasaki GJH. Effect of permeability on implicit-texture foam model parameters and the limiting capillary pressure. Energy Fuels 2015;29(5):3011–8.
- [60] Lotfollahi M, Varavei A, Delshad M, Farajzadeh R, Pope GA. A four-phase flow model to simulate chemical EOR with gas (SPE 173322). Society of Petroleum Engineers - SPE Reservoir Simulation Symposium. 2015. p. 2190–222.
- [61] Groenenboom J, Berhad SS, Kechut NI, Mar-Or A. Foam-assisted WAG: injection strategies to optimize performance (SPE 186991). Soc. Pet. Eng. - SPE/IATMI Asia Pacific Oil Gas Conf. Exhib. 2017. 2017.
- [62] Ahmad I, Awang M, Sufian S, Irfan Khan M, Mumtaz M. Effect of ball milling of fly ash particle size on foam stabilization for EOR applications. J Teknol 2016;78(6–7):115–9.
- [63] Lau HC, Yu M, Nguyen QP. “Nanotechnology for oilfield applications: challenges and impact (SPE 183301). Society of Petroleum Engineers - Abu Dhabi International Petroleum Exhibition and Conference 2016. 2016.
- [64] Van Der Merwe EM, Prinsloo LC, Mathebula CL, Swart HC, Coetsee E, Doucet FJ. Surface and bulk characterization of an ultrafine South African coal fly ash with reference to polymer applications. Appl Surf Sci 2014;317:73–83.
- [65] Attarhamed F, Zoveidavianpoor M, Jalilavi M. The incorporation of silica nanoparticle and alpha olefin sulphonate in aqueous CO₂ foam: investigation of foaming behavior and synergistic effect. Pet Sci Technol 2014;32(21):2549–58.
- [66] Pugh RJ. Foaming, foam films, antifoaming and defoaming. Adv Colloid Interface Sci 1996;64:67–142.
- [67] Fameau AL, Salonen A. Effect of particles and aggregated structures on the foam stability and aging. Comptes Rendus Physique, vol. 15. Elsevier Masson SAS; 2014. p. 748–60.
- [68] Yekeen N, et al. A comprehensive review of experimental studies of nanoparticles-stabilized foam for enhanced oil recovery. J Pet Sci Eng 2018;164(December 2017):43–74.
- [69] Yekeen N, Idris AK, Manan MA, Samin AM, Risal AR, Kun TX. Bulk and bubble-scale experimental studies of influence of nanoparticles on foam stability. Chin J Chem Eng 2017;25(3):347–57.
- [70] Hamza MF, Sinnathambi CM, Merican Z, Merican A, Soleimani H, Stephen KD. Effect of SiO₂ on the foamability, thermal stability and interfacial tension of a novel nano-fluid hybrid surfactant. Int J Adv Appl Sci 2018;5(1):113–22.
- [71] Chea TB, Akhir NAM, Idris AK. Investigation on the effect of types of nanoparticles and temperature on nanoparticles-foam stability 2017 Proc. Int. Conf. Ind. Eng. Oper. Manag. 2018. p. 365–72.
- [72] Guo F, He J, Johnson PA, Aryana SA. Stabilization of CO₂ foam using by-product fly ash and recyclable iron oxide nanoparticles to improve carbon utilization in EOR processes. Sustain Energy Fuels 2017;1(4):814–22.
- [73] Horozov TS. Foams and foam films stabilised by solid particles. Curr Opin Colloid Interface Sci 2008;13(3):134–40.
- [74] Vatanparast H, Samiee A, Bahramian A, Javadi A. Surface behavior of hydrophilic silica nanoparticle-SDS surfactant solutions: I. effect of nanoparticle concentration on foamability and foam stability. Colloids Surf A Physicochem Eng Asp 2017;513:430–41.
- [75] Mohd TAT, et al. Relationship between foamability and nanoparticle concentration of carbon dioxide (CO₂) foam for enhanced oil recovery (EOR). Appl Mech Mater 2014;548–549:67–71.
- [76] Singh R, Mohanty KK. Synergy between nanoparticles and surfactants in stabilizing foams for oil recovery. Energy Fuels 2015;29(2):467–79.
- [77] Risal AR, Manan MA, Yekeen N, Azli NB, Samin AM, Tan XK. Experimental investigation of enhancement of carbon dioxide foam stability, pore plugging, and oil recovery in the presence of silica nanoparticles. Pet Sci 2019;16(2):344–56.
- [78] Murphy MJ. Experimental analysis of electrostatic and hydrodynamic forces affecting nanoparticle retention in porous media Master Thesis University of Texas at Austin; 2012.
- [79] Heller JP, Lien CL, Kuntamukkula MS. Foamlike dispersions for mobility control in CO₂ floods (SPE 11233). Soc Pet Eng J 1985;25(4):603–13.
- [80] Gong J, et al. Laboratory investigation of liquid injectivity in surfactant-alternating-gas foam enhanced oil recovery. Transp Porous Media 2019(August 2018):26–8.
- [81] Hussain AAA, Vincent-Bonnieu S, Kamarul Bahrim RZ, Pilus RM, Rossen WR. Impact of crude oil on pre-generated foam in porous media. J Pet Sci Eng 2019:106628.
- [82] Sheng JJ. Foams and their applications in enhancing oil recovery. Enhanced oil recovery field case studies. Elsevier Inc.; 2013. p. 251–80.
- [83] Simjoo M, Zitha PLJ. New insight into immiscible foam for enhancing oil recovery. Flow Transp Subsurf Environ 2018:91–115.
- [84] Ibrahim F, Abdulkerim. History matching with reduced parameterization and fast streamline-based sensitivities Master Thesis Norway: Department of Mathematics, University of Bergen; 2012.
- [85] Zhang K. “Experimental and numerical investigation of oil recovery from bakken formation by miscible CO₂ injection (SPE 184486),” In: Proc. - SPE Annu. Tech. Conf. Exhib., pp. 1–23, 2016.
- [86] Baker RO, Chugh S, McBurney C, McKishnie R. History matching standards; quality control and risk analysis for simulation. Canadian international petroleum conference 2006, CIPC 2006. 2006.
- [87] Salerl NG. “Reservoir Performance Forecasting: Acceleration by Parallel Planning (SPE 25151),” 1993.
- [88] Sun L, Wang B, Pu W, Yang H, Shi M. The effect of foam stability on foam flooding recovery. Pet Sci Technol Jan. 2015;33(1):15–22.